# Two-sphere low-Reynolds-number propeller

Ali Najafi[1,*] and Rojman Zargar[2]
[1]*Department of Physics, Zanjan University, Zanjan 313, Iran*
[2]*Institute for Advanced Studies in Basic Sciences (IASBS), P.O. Box 45195-1159, Zanjan 45195, Iran*
(Received 7 January 2010; revised manuscript received 12 May 2010; published 4 June 2010)

A three-dimensional model of a low-Reynolds-number swimmer is introduced and analyzed in this Brief Report. This model consists of two large and small spheres connected by two perpendicular thin rods. The geometry of this system is motivated by the microorganisms that use a single tail to swim; the large sphere represents the head of microorganism and the small sphere resembles its tail. Each rod changes its length and orientation in a nonreciprocal manner that effectively propels the system. Translational and rotational velocities of the swimmer are studied for different values of parameters. Our findings show that by changing the parameters we can adjust both the velocity and the direction of motion of the swimmer.

DOI: 10.1103/PhysRevE.81.067301 PACS number(s): 47.15.G−, 87.19.ru, 45.40.Ln

## I. INTRODUCTION

The propulsive motion of artificial and biological micron-scale objects is an interesting problem at low-Reynolds-number hydrodynamics. In this condition the dynamics is dominated by viscous forces. Examples of these micron-scale objects include biological microorganisms such as bacteria and also man made microswimmers, useful to operate at microfluidic investigations [1].

Propulsive motion at low Reynolds number is subject to the *scallop theorem* [2]. At small scales, where the Reynolds number is very low, the governing hydrodynamic equations, i.e., the Stokes and continuity equations, are linear and invariant under time reversal [3]. Any reciprocal shape deformation retraces its trajectory and the system stays back at the point where it started. In order to achieve a net translational displacement, the system should perform the body deformations in a nonreciprocal manner. As mentioned by Purcell a low-Reynolds-number propeller must have at least two internal degrees of freedom and he proposed a three-link swimmer. The detailed motion of Purcell's swimmer was examined by Becker *et al.* where it was shown that Purcell's system could swim and its dynamical properties were calculated [4]. Inspired by Purcell's system, a low-Reynolds-number swimmer constructed by three linked spheres was introduced and analyzed by Najafi *et al.* [5] and experimentally realized by Leoni *et al.* [6]. After Purcell's proposal there have been considerable scientific efforts in designing artificial swimmers. Such swimmers would be useful in developing microfluidic experiments. Furthermore, progresses in assembling microswimmers show the possibility of using micromachines inside the biological cells for noninvasive therapeutic treatments [7]. On the other hand, there are many theoretical works devoted to the study of different aspects in the motion of biological microorganisms at low-Reynolds-number condition [8–12]. Such interests include sperm swimming, metachronal waves in cilia, *E. Coli* chemotaxis, and coupling mediated by hydrodynamic interaction between nearby microorganisms [13,14]. For a review of recent progress on low-Reynolds-number hydrodynamics of microorganisms, see, for example, the review paper by Lauga and Powers [15].

Our first aim in this Brief Report is to present a simplified model that captures the characteristics of a swimming biological organism like a bacterium. Dipolar far velocity field and asymmetric shape, corresponding to the head-tail geometry of the organisms, are two important features of microswimmers. We model these systems by considering two spheres with different radii that are changing their separation. We will study the translational and angular motions of this system.

## II. TWO-SPHERE MODEL

Figure 1 shows the schematic geometry of a model swimmer composed of two spheres. As shown in this figure two small and large spheres with radii $a$ and $R$ are connected by two perpendicular and negligible diameter rods. Let denote the lengths of long and short rods by $L$ and $l$, respectively. The connection is established in a way that the angle between two rods is fixed to $\frac{\pi}{2}$ while the relative angular position of small rod with respect to the large sphere can be varied. Additionally, we assume that the length of the long rod can be dynamically changed. In this case, the system will have two internal degrees of freedom: the length of the long rod $L(t)$ and the rotational angle of the short rod $\phi(t)$.

The geometry which we are introducing here resembles the body shape of a bacterium with a single flagellum or cilium. Bacteria use beating patterns in their tails to move. The small sphere in our two-sphere model acts as a beating tail and the large sphere resembles the head of animal. The minimum condition for swimming at low Reynolds number can be achieved in our three-dimensional model. By changing the length of long rod and the angle of small one in a prescribed form, we are able to choose the motion which breaks the time-reversal symmetry, the necessary condition for translational motion, and consequently propel the system.

As an example for the internal motion of the system, we let the angle $\phi(t)$ increase with constant angular velocity and the length of long rod change periodically around an average length. The explicit form of this motion is given by $L(t)$

*najafi@znu.ac.ir

 

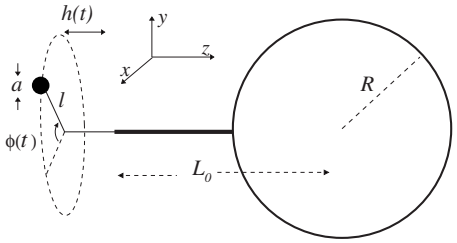


FIG. 1. Schematic showing the geometry of a two-sphere swimmer. Two large and small spheres are connected through two perpendicular rods, one with fixed but the other with variable length. The short rod is rotating around the long rod. This model system resembles the motion of a bacterium that has a single tail.

$=L_0+h_0\cos(\omega_L t-\phi_0)$ and $\phi(t)=\omega_\phi t$. In this case, the position vector of the small sphere, seen in the reference frame that is comoving with the large sphere, is given by

$$\mathbf{X}_0=(l\cos\phi(t), l\sin\phi(t), L_0+h(t)), \tag{1}$$

where $l$ is the length of the small rod and $L_0$ represents the average length of the long rod. Figure 2 shows a typical real-space trajectory of the small sphere that is seen in the reference frame comoving with the large sphere. Different choices for $\omega_L$ and $\omega_\phi$ correspond to different forms of the internal motion. For $\omega_\phi/\omega_L=m=p/q$ with $p$ and $q$ as two positive integer numbers, we see that the paths in the $(h,\phi)$ space are closed loops. One should note that the phase space of internal motion $[(h,\phi)$ space$]$ is the surface of a cylinder. The axial direction on the cylinder represents the $h$ direction and the azimuthal angle is shown by the transverse direction on the cylinder. For $m<1$, the phase-space trajectory is a closed curve which traces exactly one complete turn around the cylinder, while for $m\geq 1$ the trajectory is a closed loop that turns many times around the cylinder. In both cases, the geometry of the closed curves in the cylindrical-shape phase space is an example of nonreciprocal motion that can generate a net translational motion.

## III. POINT FORCE NEAR A RIGID SPHERE

At zero Reynolds number the Stokes equations govern the dynamics of fluid. The solution of the Stokes equation for a point force singularity is formulated in terms of the Green's function and is called Stokeslet. For a point force singularity with strength $\mathbf{f}$ located at point $\mathbf{X}_0$, the velocity field generated in the fluid is given by $\mathbf{u}(\mathbf{X})=\frac{1}{8\pi\eta}G(\mathbf{X},\mathbf{X}_0)\cdot\mathbf{f}$, where $\eta$ is the viscosity of the fluid. Oseen derived the explicit form of the Green's function $G$ for an infinite flow that is bounded internally by a solid sphere with radius $R$ [16]. For the explicit form of this solution, we refer to the original paper by Oseen. As it is manifested by Oseen's solution, the flow field due to a point force in the presence of a solid sphere can be regarded as the flow of the original point force and the flow due to the singular parts that are located at an image position inside the sphere. The location of the image point inside the sphere is given by its position vector, $\mathbf{X}_0^*=(R^2/X_0^2)\mathbf{X}_0$, relative to the sphere's center.

As argued by Higdon the total force acting by a point force on fluid bounded by a no-slip sphere is equivalent to the total Stokeslet strength [17]. The total Stokeslet strength includes the image point force inside the sphere. For a point force $\mathbf{f}$, the image point force is defined by $\mathbf{f}_I=(c_r\mathbf{f}_r+c_t\mathbf{f}_t)$ where the radial and tangential components of this image force are given by $\mathbf{f}_r=\mathbf{f}\cdot\mathbf{X}_0/X_0$, $\mathbf{f}_t=\mathbf{f}-\mathbf{f}_r$. Here, two coefficients $c_r$ and $c_t$ are given by

$$c_r=-\frac{3}{2}\frac{R}{X_0}+\frac{1}{2}\frac{R^3}{X_0^3},\quad c_t=-\frac{3}{4}\frac{R}{X_0}-\frac{1}{4}\frac{R^3}{X_0^3}. \tag{2}$$

In the next section we will use these results for analyzing the motion of two-sphere system.

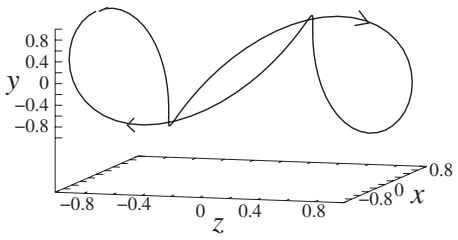


FIG. 2. Trajectory of the small sphere seen in the frame of reference that is comoving with large sphere. Here, we chose $h_0=1$ and $\omega_\phi/\omega_L=2$.

## IV. TWO-SPHERE DYNAMICS

In this section we will develop the dynamical equations for two-sphere system. To simplify the equations We will assume that the radius of small sphere is much smaller than the radius of large sphere $(a\ll R)$. We further assume that $a$ is smaller than the characteristic distance between the spheres. With this approximation the velocity field of the system is described by the velocity field of a point force that is moving near a rigid sphere. This simplification allows us to use the results of the preceding section and derive simpler dynamical equations of the system. However, one should note that the finite-size effect of the small sphere can be systematically considered by Faxen's theorem [18].

To obtain the swimming velocity of the system we work in the reference frame that is comoving and rotating with the large sphere. In this coordinate system the velocity of the fluid at infinity is the swimming velocity. Denoting the swimming velocity of the system by $V$ and its angular velocity by $\Omega$, we can express the velocity field of the fluid at a general point $\mathbf{X}$ as

$$\mathbf{u}(\mathbf{X})=-\mathbf{V}-\mathbf{\Omega}\times\mathbf{X}+M\cdot\mathbf{V}+\mathbf{\Omega}\times\mathbf{m}+G\cdot\mathbf{f}, \tag{3}$$

where the tensor $M$ and vector $\mathbf{m}$ give the flow field due to the translational and rotational motions of a moving sphere. These quantities are given by

$$M=\frac{3}{4}\frac{R}{X}\left[\mathbf{I}+\frac{\mathbf{XX}}{X^2}\right]+\frac{1}{4}\frac{R^3}{X^3}\left[\mathbf{I}-3\frac{\mathbf{XX}}{X^2}\right],\quad \mathbf{m}=\frac{R^3}{X^3}\mathbf{X}. \tag{4}$$

In the absence of external force and torque, the swimmer is force and torque free. Therefore, we require the total force and torque acting on the fluid by the system to be zero. Including the point force and its image counterpart and add-

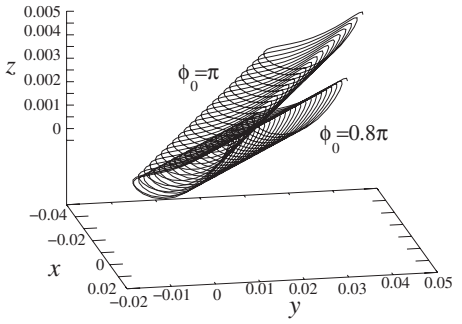


FIG. 3. The trajectory of the swimmer in the $(x,y,z)$ space is plotted for two different values of $\phi_0$. Other parameters are $R=1$, $a=0.5$, $L_0=4$, $h_0=0.1$, $l=0.3$, and $\omega_\phi=2\omega_l=1$. Line shows the real path of the large sphere. The swimmer starts its motion from the initial state where the large sphere is located at the origin and the long rod is orientated along the $-\hat{z}$ direction. As one can see, the overall swimming direction can be varied by changing the parameters of the system. Average orientation of the long rod which is not shown here is along the average swimming direction.

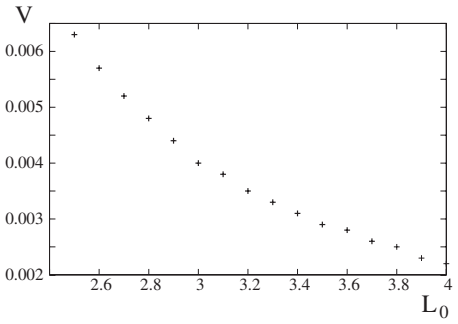


FIG. 4. Average swimming velocity is plotted in terms of the length of long rod. Other parameters are set to $R=1$, $a=0.5$, $\phi_0=0$, $h_0=0.1$, $l=0.3$, and $\omega_\phi=\omega_l=1$.

ing the contributions due to the translational and rotational motions of large sphere, we arrive at the following force and torque balance equations:

$$\mathbf{f}+\mathbf{f}_I+6\pi\eta R\mathbf{V}=0,$$

$$\mathbf{X}_0\times\mathbf{f}_t-\frac{R^3}{X_0^3}\mathbf{X}_0\times\mathbf{f}_t+8\pi\eta R^3\mathbf{\Omega}=0. \tag{5}$$

The fluid velocity field at the location of small sphere is subject to the boundary condition $\mathbf{u}(\mathbf{X}_0)=\dot{\mathbf{X}}_0$. Together with this boundary condition, the above equations make a complete set of dynamical governing equations for the swimmer.

To solve the dynamical equations for the system, we can use the force and torque balance conditions and obtain a set of equations which relate the different components of the translational or angular velocities of the system to the component of the vector $\dot{\mathbf{X}}_0$ in the following matrix form:

$$\mathbf{V}=\mathbf{A}\mathbf{C}^{-1}\dot{\mathbf{X}}_0,$$

$$\mathbf{\Omega}=\mathbf{B}\mathbf{C}^{-1}\dot{\mathbf{X}}_0, \tag{6}$$

where the details for of the matrix elements $[A]_{ij}=a_{ij}$, $[B]_{ij}=b_{ij}$, and $[C]_{ij}=c_{ij}$ are given in the Appendix.

## V. RESULTS AND DISCUSSION

In this section we will present the numerical solution for the governing equations and obtain the real-space trajectory of the swimmer. For this purpose we plot the trajectory of large sphere. For the prescribed internal motion given by Eq. (1) and a special choice of parameters, we have plotted in Fig. 3 the space trajectory of the large sphere. As one can distinguish, the trajectory is a helical-shaped path with an overall translational movement in each turn. The different characteristics of the trajectory, preferred direction, average swimming velocity, and the effective radius of the helix can be controlled by the geometrical as well as dynamical parameters of the swimmer.

The average orientation of the long rod, which is not shown in the figure, is in the direction of the longitudinal axis of the helix. This is achieved by numerically solving for the rotational velocity. Controlling and adjusting the dynamical behavior of the swimmer are of prime importance in designing artificial micromachines. Here, we see that by changing the parameters of the system we can do this favor. In Fig. 3, we have shown that the overall swimming direction is sensitive to the initial phase $\phi_0$. Additionally and as another example, in Fig. 4, we have shown that by changing $L_0$, the length of long rod, the average swimming velocity can be changed.

As the geometry of the two-sphere swimmer is not symmetric, the far-field distribution of fluid velocity at the leading order of approximation resembles a velocity field of a single force dipole. This is the main characteristic of most swimming microorganisms with a dipolelike velocity pattern.

In summary, inspired by bacterium swimming, we proposed and analyzed a swimmer, constructed by two joint spheres. We have shown that this simple three-dimensional swimmer is a model for a low-Reynolds-number propeller that captures a number of dynamical features in microorganisms. It will be interesting to use this model swimmer and study many interesting problems such as the hydrodynamic interaction between such swimmers, the effects due to the confinement in the bounded fluids, and also chemotaxis phenomena. Inspired by the colonies of microorganisms, we are extending our model to investigate the hydrodynamic interaction in an ensemble of two-sphere swimmers.

## APPENDIX: MATHEMATICAL DETAILS

Here, we present the explicit form of the matrix elements $a_{ij}$, $b_{ij}$, and $c_{ij}$ which were introduced in the text,

$$a_{ii}=-\frac{1}{6\pi\eta R}\left[(1+c_t)+(c_r-c_t)\left(\frac{X_{0i}^2}{X_0^2}\right)\right],$$

$$a_{ij}=a_{ji}=-\frac{1}{6\pi\eta R}(c_r-c_t)\left(\frac{X_{0i}X_{0j}}{X_0^2}\right)\quad\text{for } i\neq j,$$

$$b_{ii} = 0,$$

$$b_{ij} = -b_{ji} = \frac{1}{8\pi\eta R^3}\left(1 - \frac{R^3}{X_0^3}\right)X_{0k} \quad \text{for } i \neq j \neq k,$$

$$c_{11} = (M_{xx} - 1)a_{11} + M_{xy}a_{21} + M_{xz}a_{31} + (m_z - z_0)b_{21} - (m_y - y_0)b_{31} + G_{xx},$$

$$c_{12} = (M_{xx} - 1)a_{12} + M_{xy}a_{22} + M_{xz}a_{32} - (m_y - y_0)b_{32} + G_{xy},$$

$$c_{13} = (M_{xx} - 1)a_{13} + M_{xy}a_{23} + M_{xz}a_{33} + (m_z - z_0)b_{23} + G_{xz},$$

$$c_{21} = M_{yx}a_{11} + (M_{yy} - 1)a_{21} + M_{yz}a_{31} + (m_x - x_0)b_{31} + G_{yx},$$

$$c_{22} = M_{yx}a_{12} + (M_{yy} - 1)a_{22} + M_{yz}a_{32} + (m_x - x_0)b_{32} - (m_z - z_0)b_{12} + G_{yy},$$

$$c_{23} = M_{yx}a_{13} + (M_{yy} - 1)a_{23} + M_{yz}a_{33} - (m_z - z_0)b_{13} + G_{yz},$$

$$c_{31} = M_{zx}a_{11} + M_{zy}a_{21} + (M_{zz} - 1)a_{31} - (m_x - x_0)b_{21} + G_{zx},$$

$$c_{32} = M_{zx}a_{12} + M_{zy}a_{22} + (M_{zz} - 1)a_{32} + (m_y - y_0)b_{12} + G_{zy},$$

$$c_{33} = M_{zx}a_{13} + M_{zy}a_{23} + (M_{zz} - 1)a_{33} + (m_y - y_0)b_{13} - (m_x - x_0)b_{23} + G_{zz}.$$


[1] H. Bruss, *Theoretical Microfluidics* (Oxford University Press, Oxford, 2008).
[2] E. M. Purcell, Am. J. Phys. **45**, 3 (1977).
[3] J. Happel and H. Brenner, *Low Reynolds Number Hydrodynamics* (Prentice-Hall, Englewood Cliffs, NJ, 1965).
[4] L. E. Becker, S. A. Koehler, and H. A. Stone, J. Fluid Mech. **490**, 15 (2003).
[5] A. Najafi and R. Golestanian, Phys. Rev. E **69**, 062901 (2004); R. Zargar, A. Najafi, and M. F. Miri, *ibid.* **80**, 026308 (2009).
[6] M. Leoni, J. Kotar, B. Bassetti, P. Cicuta, and M. Lagomarsino, Soft Matter **5**, 472 (2009).
[7] K. Ishiyama, M. Sendoh, A. Yamazaki, and K. I. Arai, Sens. Actuators, A **91**, 141 (2001).
[8] M. Ramia, D. L. Tullock, and N. Phan-Thien, Biophys. J. **65**, 755 (1993).
[9] W. R. DiLuzio *et al.*, Nature (London) **435**, 1271 (2005).
[10] B. U. Felderhof, Phys. Fluids **18**, 063101 (2006).
[11] D. J. Earl *et al.*, J. Chem. Phys. **126**, 064703 (2007).
[12] J. P. Hernandez-Ortiz, C. G. Stoltz, and M. D. Graham, Phys. Rev. Lett. **95**, 204501 (2005).
[13] H. C. Berg, *E. Coli in Motion* (Springer-Verlag, New York, 2004).
[14] B. M. Friedrich and F. Julicher, Proc. Natl. Acad. Sci. U.S.A. **104**, 13256 (2007).
[15] E. Lauga and T. R. Powers, Rep. Prog. Phys. **72**, 096601 (2009).
[16] C. W. Oseen, *Neuere Methoden und Ergebniss in der Hydrodynamik* (Akademishe Verlagsgesellschaft, Leipzig, 1927).
[17] J. J. L. Higdon, J. Fluid Mech. **90**, 685 (1979).
[18] Y. W. Kim and R. R. Netz, J. Chem. Phys. **124**, 114709 (2006).